Eur. J. Org. Chem. **2013** · © WILEY-VCH Verlag GmbH & Co. KGaA, 69451 Weinheim, 2013 · ISSN 1099–0690

SUPPORTING INFORMATION

DOI: 10.1002/ejoc.201300146
Title: Epicoccolides: Antimicrobial and Antifungal Polyketides from an Endophytic Fungus *Epicoccum* sp. Associated with *Theobroma cacao*
Author(s): Ferdinand Mouafo Talontsi, Birger Dittrich, Anja Schüffler, Han Sun, Hartmut Laatsch*

Table of contents:

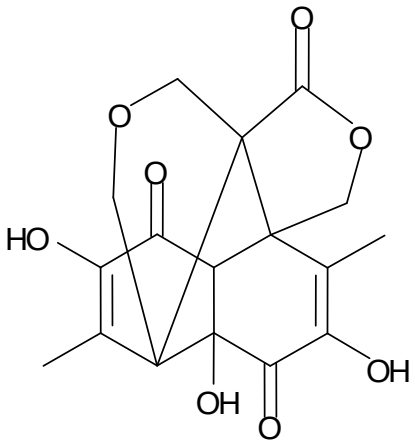

Figure S1. Epicolactone (**1**) in "naphthalene view"

Single-Crystal X-ray structure analysis

Single crystals were grown from a methanol solution by evaporation of the solvent. A suitable specimen was selected and mounted on a Bruker three circle diffractometer using NVH oil. The diffractometer was equipped with a SMART 6000 CCD area detector and a CuKα rotating anode generator. The diffraction data were collected at a temperature of 100 K with a nitrogen gas-stream cooling device. Due to good crystal quality and scattering power, data were collected to the edge of the CuKα Ewald sphere with a high completeness of 97%, a redundancy of 4.9, and a low internal R value of 2.1%. A total number of 15159 reflections were collected. The raw data were integrated with SAINT, version 7.61A,[1] and an empirical absorption correction with SADABS, Version 2008/2,[2] was applied in turn. SADABS was also used to merge the data and to generate SHELX and XD format hkl-files. The structure was solved by direct methods (SHELXS-97[3]), and initially refined against all data by full-matrix least-squares methods on F^2 (SHELXL-97). SHELXLE[4] was used as the refinement GUI. All non-hydrogen atoms were refined with anisotropic displacement parameters. Rigid bond, distance or other restraints were not required in the refinement of the structure. Since valence electron density was systematically visible on most covalent bonds in the difference Fourier map after convergence in the SHELXLE-GUI, we decided that using non-spherical scattering factors ("invarioms" from invariant, *i.e.* transferable, pseudoatoms[5]) of the invariom database[6] would most likely improve the structure in terms of the *R*-Factor and the physical meaning of the anisotropic displacement parameters. We therefore used the SHELXL independent-atom model (IAM) to initiate a non-spherical atom refinement with the program XDLSM,[7] which incorporates the rigid pseudoatom scattering-factor formalism from Hansen and Coppens.[8] Scattering factor assignment and the correct orientation of the

local-atomic coordinate system was achieved by evoking the program INVARIOMTOOL.[9,10] A list of model compounds from which the scattering factors were extracted is given below. After invariom refinement, the *R*-factor dropped by more than one percent, from 3.79% to 2.68%. Refinement in XDLSM was done on *F* using all reflections with $I > 3\,\sigma(I)$, which were 2958 out of the 3048 measured unique reflections. Concerning hydrogen-atom treatment, H-atoms were initially constrained using suitable AFIX commands in SHELXL. The relative hydrogen geometry from SHELXL was subsequently maintained: during the initial scale-factor refinement after transfer to the XD-system files, the bond distances to H-atoms were elongated to values from the respective model compounds from the invariom database with RESET BOND commands generated by INVARIOMTOOL, keeping the angles to the calculated values from SHELXL. Subsequent hydrogen-atom shifts in the least-squares procedure were constrained to follow the parent atom on which the hydrogen atoms were riding. The required CON cards for XDLSM were also generated by INVARIOMTOOL. This procedure led to optimal *R*-factors for the title compound. Concerning the physical meaning of the anisotropic displacement parameters, the use of invariom led to a significant reduction in most individual and the average values of the difference of the mean-square displacement amplitudes (DMSDA) as quantified with the Hirshfeld test.[10] Individual values from IAM refinement with XDLSM led to, on average, values of twice the size (8.6 $Å^2$) than for invariom refinement with an average of 4.3 $Å^2$. In addition, no DMSDA value violates the Hirshfeld test after invariom refinement, whereas in the IAM, 9 values out of 30 do (see below). An ORTEP-plot of the structure after invariom refinement is also given in Figure S3.

Table S1: Hirshfeld-test[10] result for Epicolactone (**1**)

Bond	DMSDA (invarioms)	DMSDA (IAM)
O(1)---C(2)	-3	15
O(2)---C(3)	1	0
O(3)---C(8)	5	16
O(4)---C(14)	1	0
O(4) ---C(15)	4	-5
O(5)---C(12)	-7	7
O(5)---C(13)	-7	-6
O(6)---C(12)	5	21
O(8)---C(7)	5	27
O(9)---C(6)	9	0
O(10---C(18)	6	20
C(1)---C(2)	-3	26

C(1)---C(6)	0	0
C(1)---C(10)	-9	-19
C(2)---C(3)	-7	-23
C(3)---C(4)	3	-7
C(4)---C(5)	9	-8
C(4)---C(17)	5	2
C(5)---C(6)	1	0
C(5)---C(11)	-3	-1
C(5)---C(15)	-2	3
C(6)---C(7)	0	9
C(7)---C(8)	-3	-4
C(8)---C(9)	2	-2
C(9)---C(10)	6	-1
C(9)---C(16)	5	-2
C(10)---C(11)	2	-2
C(10)----C(13)	-2	5
C(11)---C(12)	5	22
C(11)---C(14)	-9	-5

Table S2: Model compounds used in invariom refinement

Atom:	Invariom: Model compound
O(1): O1.5c[1c1c]	from: (Z)-2-acetyl-3-hydroxybut-2-enamide
O(2): O1c1h	from: methanol
O(3): O1c1h	from: methanol
O(4): O1c1c	from: dimethylether
O(5): O1c1c	from: dimethylether
O(6): O2c	from: formaldehyde
O(8): O1.5c[1c1c]	from: (Z)-2-acetyl-3-hydroxybut-2-enamide
O(9): O1c1h	from: methanol
O(10): O1c1h	from: methanol
C(1): C1c1c1c1h	from: 2-methylpropane
C(2): C1.5o1c1c	from: (Z)-2-acetyl-3-hydroxybut-2-enamide
C(3): C2c1o1c	from: hydroxypropene
C(4): C2c1c1c	from: isobutene
C(5): C1c1c1c1c	from: 2,2-dimethylpropane
C(6): C1o1c1c1c	from: isobutanol
C(7): C1.5o1c1c	from: (Z)-2-acetyl-3-hydroxybut-2-enamide
C(8): C2c1o1c	from: hydroxypropene
C(9): C2c1c1c	from: isobutene
C(10): C1c1c1c1c	from: 2,2-dimethylpropane
C(11): C1c1c1c1c	from: 2,2-dimethylpropane
C(12): C2o1o1c	from: acetic acid
C(13): C1o1c1h1h	from: ethanol
C(14): C1o1c1h1h	from: ethanol
C(15): C1o1c1h1h	from: ethanol
C(16): C1c1h1h1h	from: ethane
C(17): C1c1h1h1h	from: ethane
C(18): C1o1h1h1h	from: methanol
H(2): H1o[1c]	from: methanol
H(3): H1o[1c]	from: methanol
H(9): H1o[1c]	from: methanol
H(10): H1o[1c]	from: methanol
H(1): H1c[1c1c1c]	from: 2-methylpropane
H(13A): H1c[1o1c1h]	from: ethanol
H(13B): H1c[1o1c1h]	from: ethanol
H(14A): H1c[1o1c1h]	from: ethanol
H(14B): H1c[1o1c1h]	from: ethanol
H(15A): H1c[1o1c1h]	from: ethanol
H(15B): H1c[1o1c1h]	from: ethanol
H(16A): H1c[1c1h1h]	from: ethane
H(16B): H1c[1c1h1h]	from: ethane
H(16C): H1c[1c1h1h]	from: ethane
H(17A): H1c[1c1h1h]	from: ethane

H(17B): H1c[1c1h1h] from:	ethane
H(17C): H1c[1c1h1h] from:	ethane
H(18A): H1c[1o1h1h] from:	methanol
H(18B): H1c[1o1h1h] from:	methanol
H(18C): H1c[1o1h1h] from:	methanol

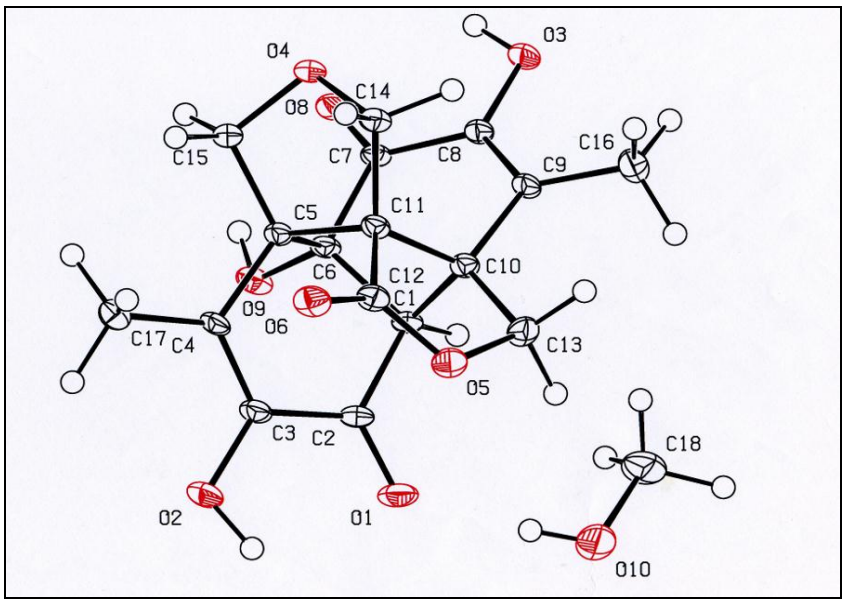

Figure S2. ORTEP-representation[11] of the X-ray crystal structure of epicolactone (**1**), with the atomic numbering scheme for non-H atoms as generated with Platon[12].

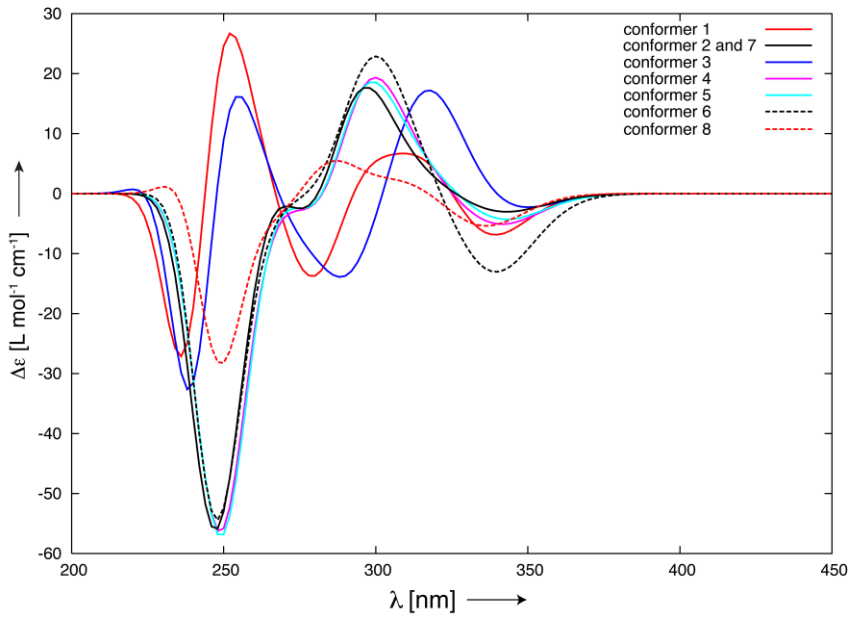

Figure S3. Calculated ECD spectra of eight conformers of epicoccolide A (**2**).

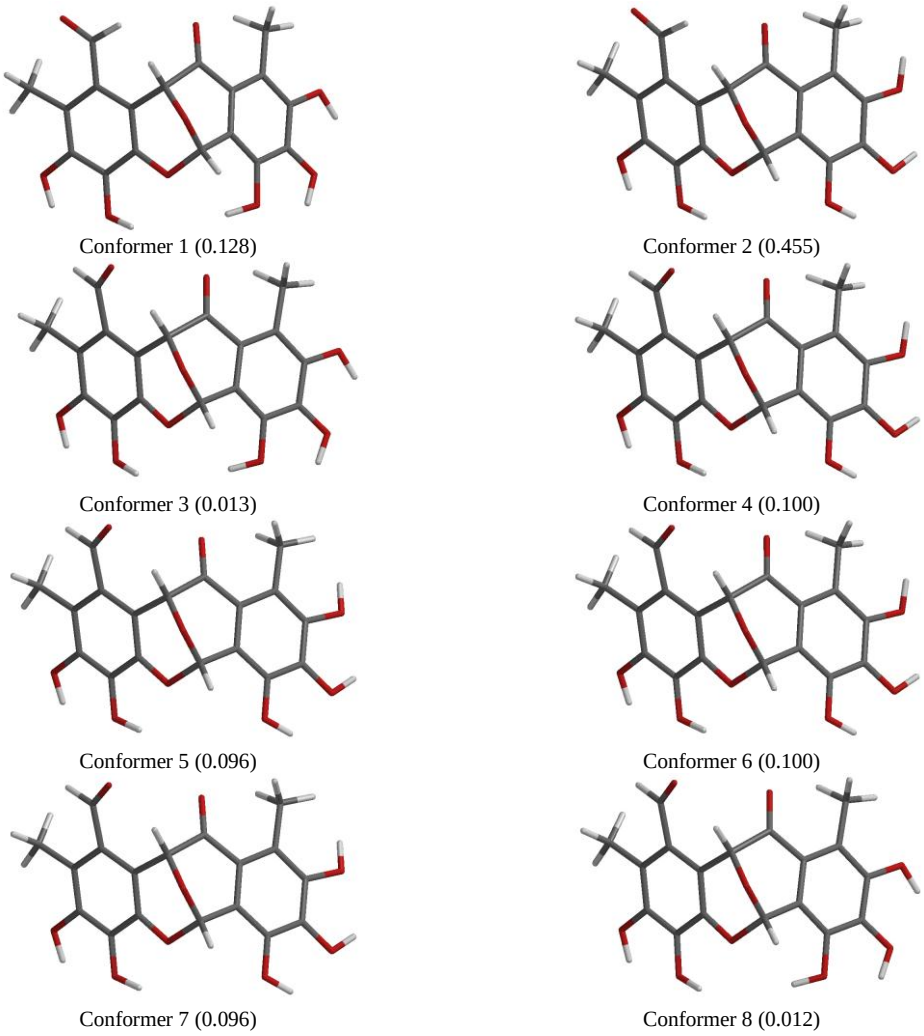

***Figure S4*:** Conformers of **2** with ground state energies less than 5 kcal above the global minimum, calculated with AM1. Values in brackets are Boltzmann populations.

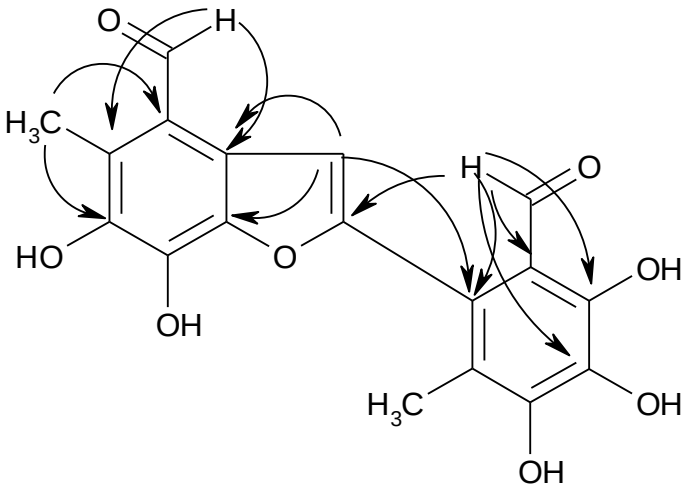

Figure S5. Selected HMBC correlations of epicoccolide B (**3**).

Table S3: ^{13}C (125 MHz) and ^{1}H NMR (300 MHz) NMR data of epicoccolide B (**3**) in DMSO-d_6.

Position	δ_C [a]	δ_H [b]	HMBC (H→C#)
2	151.6		
3	108.9	7.46 (s)	C-2, 3a, 7a, (9)
3a	122.9		
4	117.1		
5	127.5		
6	141.0		
7	136.7		
7a	142.4		
8	190.1	10.41 (s)	C-3a, 4, 5, 7a
9	124.9		
10	112.6		
11	118.7		
12	132.7		
13	151.5		
14	150.2		
15	194.7	9.48 (s)	(C-9), C-10, 12, 14
16	12.6	2.01 (s)	C-9, 11, 12,
17	11.0	2.58 (s)	C-4, 5, 6

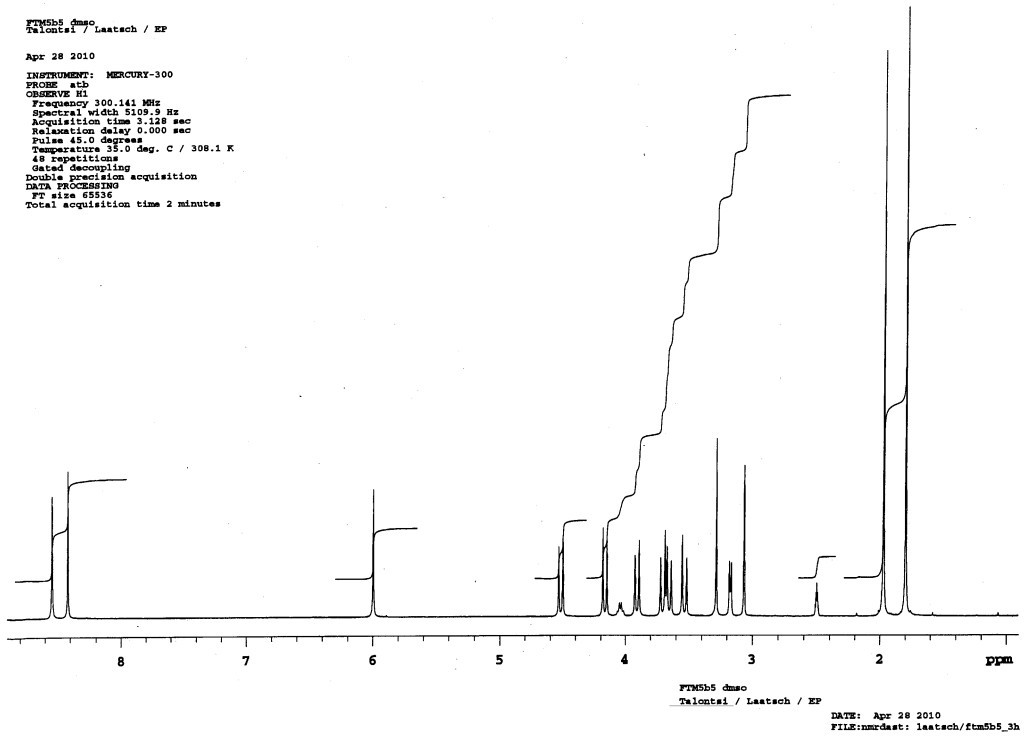

Figure S6. ^{1}H NMR spectrum (DMSO-d_6, 300 MHz) of epicolactone (**1**).

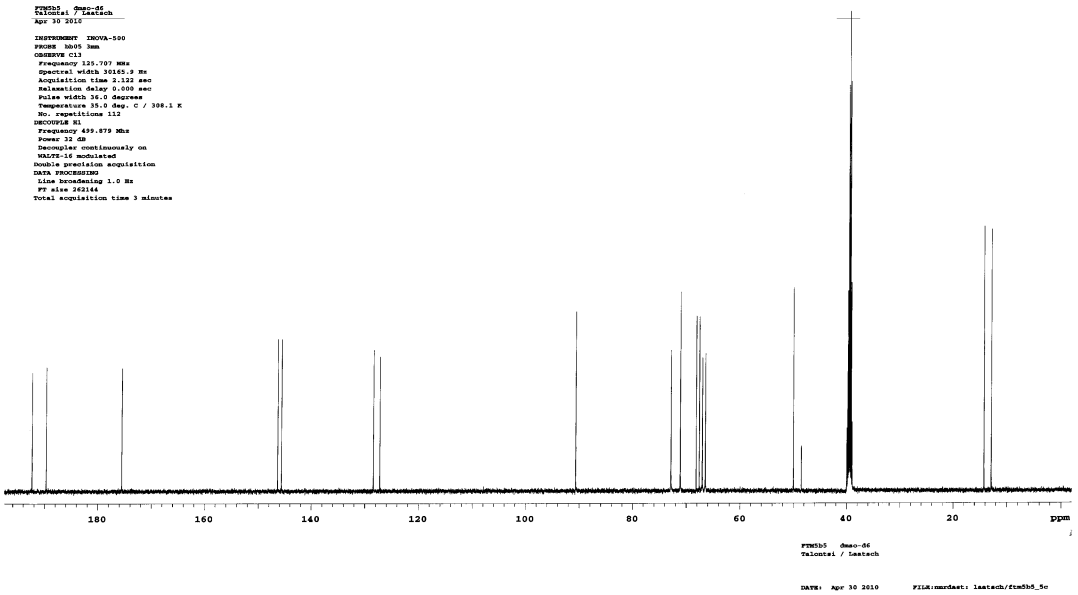

Figure S7. ^{13}C NMR spectrum (DMSO-d_6, 125 MHz) of epicolactone (**1**).

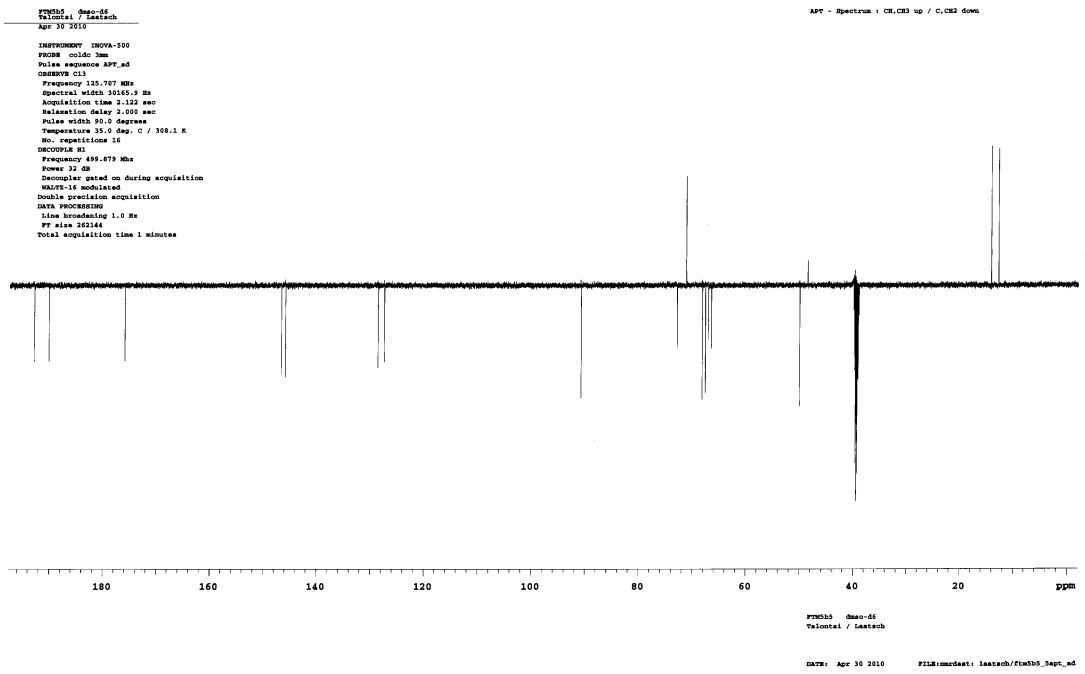

Figure S8. APT spectrum (DMSO-d_6, 125 MHz) of epicolactone (**1**).

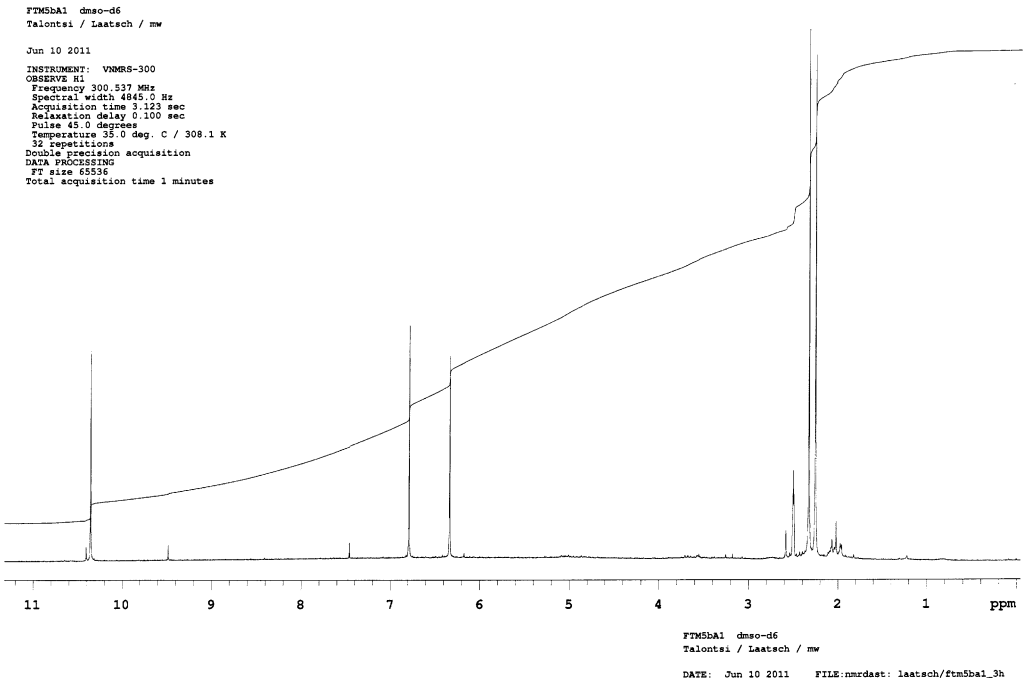

Figure S9. ^{1}H NMR spectrum (DMSO-d_6, 300 MHz) of epicoccolide A (**2**).

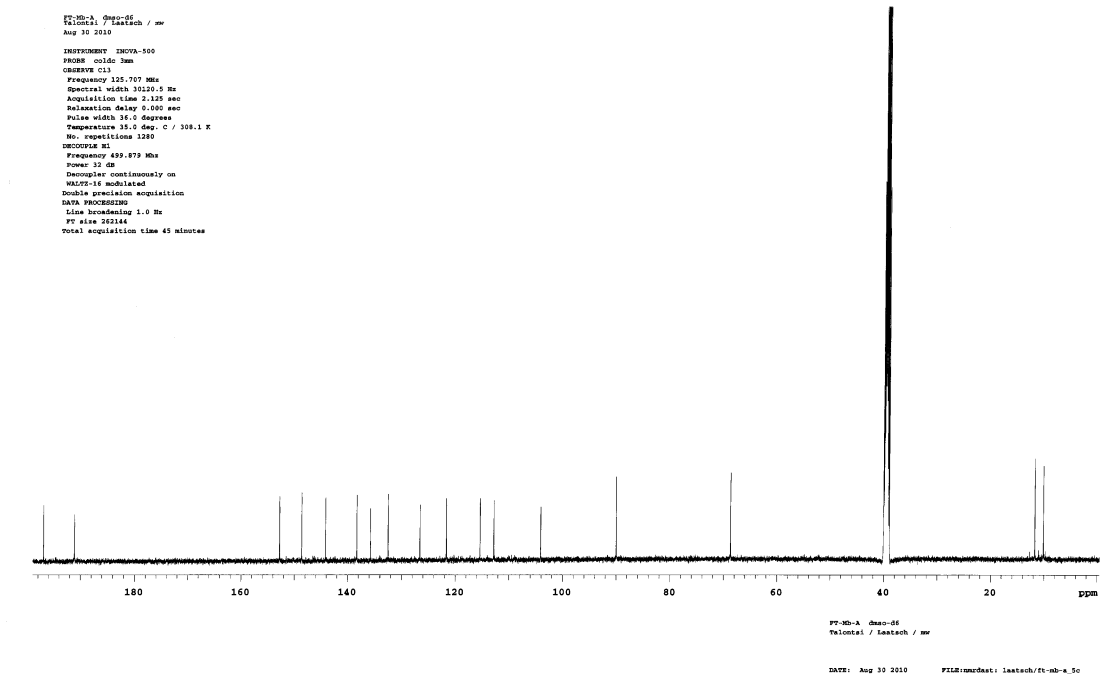

Figure S10. ^{13}C NMR spectrum (DMSO-d_6, 125 MHz) of epicoccolide A (**2**).

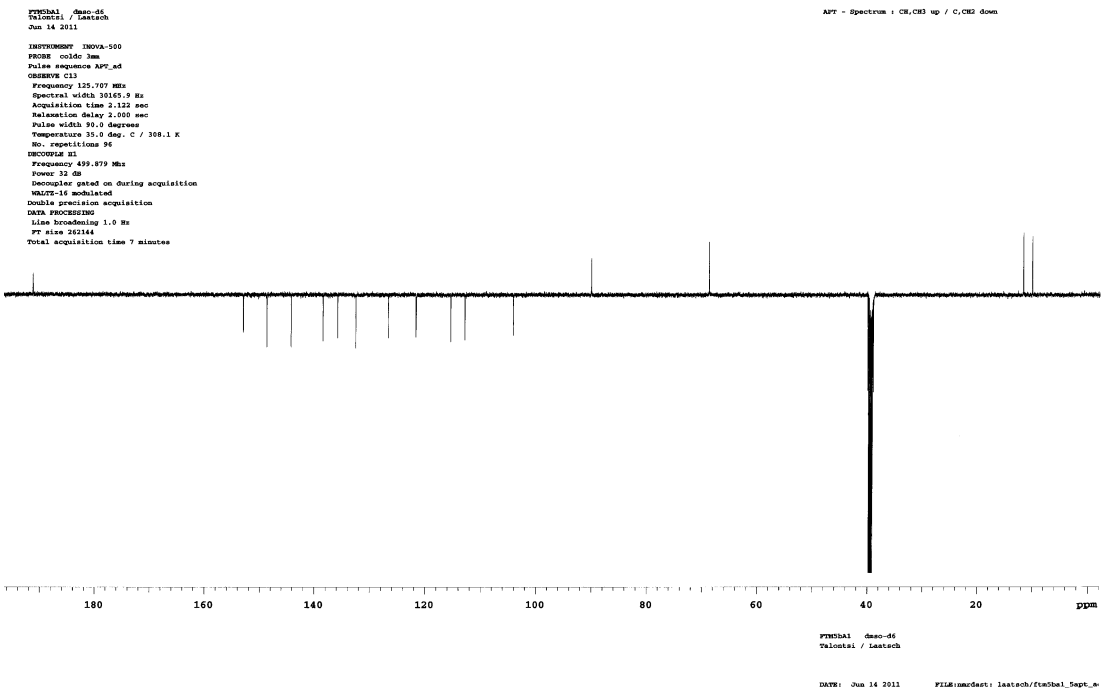

Figure S11. ^{13}C NMR APT spectrum (DMSO-d_6, 125 MHz) of epicoccolide A (**2**).

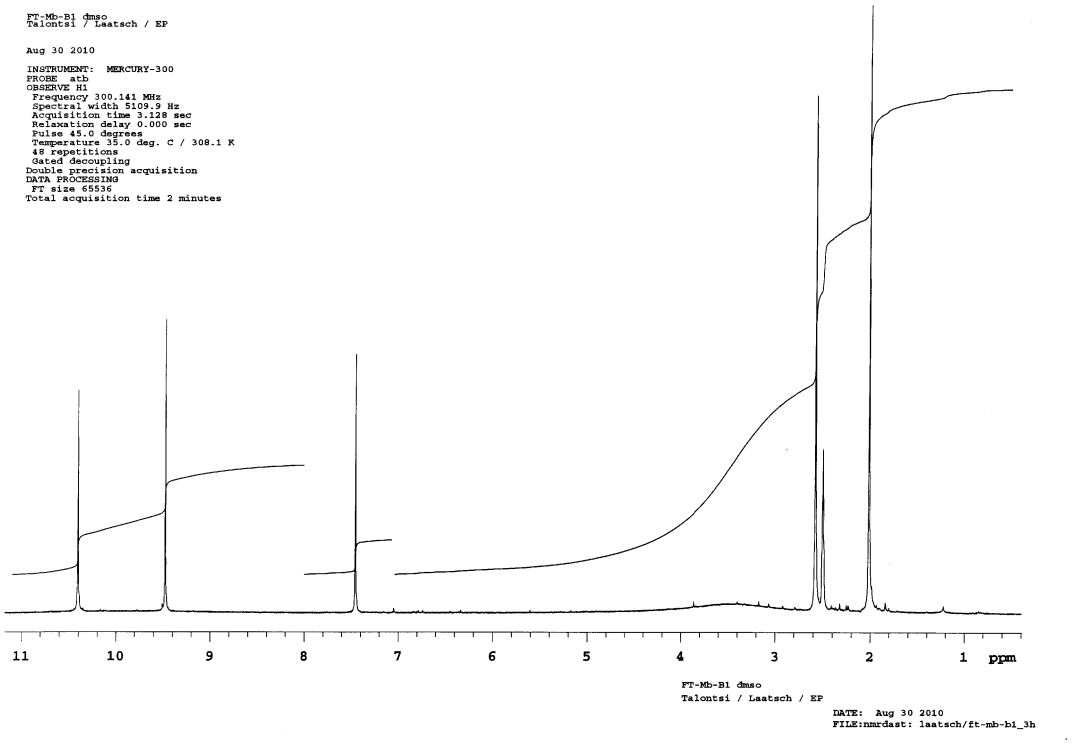

Figure S12. ^{13}C NMR spectrum (DMSO-d_6, 300 MHz) of epicoccolide B (**3**).

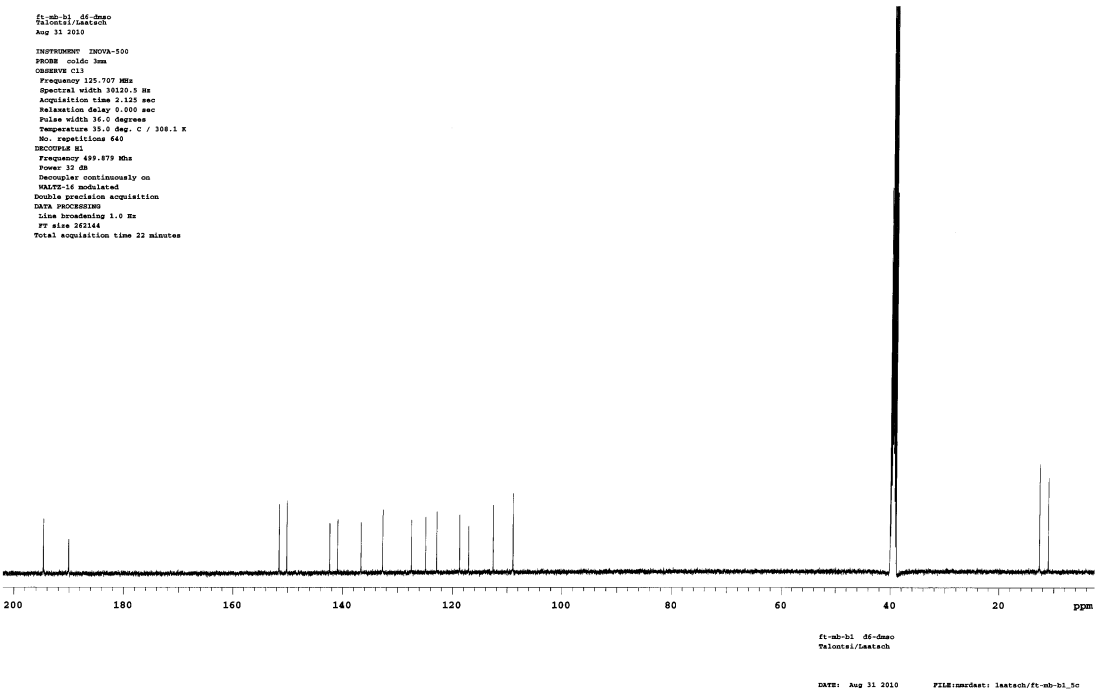

Figure S13. ^{13}C NMR spectrum (DMSO-d_6, 125 MHz) of epicoccolide B (**3**).

[1] SAINT data processing software, vers.7.61A, Bruker AXS, Madison, WI, **2008**.

[2] SADABS vers. 2008/2, G. M. Sheldrick, University of Göttingen, **2008**.

[3] G. M. Sheldrick, *Acta Cryst.* **2008**, A*64*, 112–122.

[4] C. B. Hübschle, G. M. Sheldrick, B. Dittrich, *J. Appl. Cryst.* **2011,** *44*, 1281–1284.

[5] B. Dittrich, T. Koritsánszky, P. Luger, *Angew. Chem. Int. Ed.* **2004**, *43*, 2718–2721.

[6] B. Dittrich, C. B. Hübschle, P. Luger, M. A. Spackman, *Acta Cryst.* **2006**, *D62*, 1325–1335.

[7] T. Koritsánszky, T. Richter, P. Macchi, A. Volkov, C. Gatti, S. Howard, P. R. Mallinson, L. Farrugia, Z. Su, N.K. Hansen. *XD – A Computer Program Package for Multipole Refinement and Analysis of Electron Densities from Diffraction Data.*Manual, Freie Universität Berlin, Berlin, **2003**.

[8] N. Hansen, P. Coppens, *Acta Cryst.* **1978**, *A34*, 901–921.

[9] C. B. Hübschle, P. Luger, B. Dittrich, *J. Appl. Cryst.* **2007**, *40*, 623–627.

[10] R. E. Rosenfield, K. N. Trueblood, J. D. Dunitz, *Acta Cryst.* **1978**, *A34*, 828–829; M. N. Burnett & C. K. Johnson, ORTEP-III, Oak Ridge Thermal Ellipsoid Plot Program for Crystal Structure Illustrations, Oak Ridge National Laboratory Report ORNL-6895, Oak Ridge, Tennessee, **1996**; A. L. Spek, *Acta Cryst.* **2009**, *D65*, 148–155.